

RF Properties of the 64-m-Diameter Antenna Mesh Material as a Function of Frequency

T. Y. Otoshi

Communications Elements Research Section

This article presents some accurate theoretical data on the RF properties of the perforated panels presently used as reflector surface material on the 64-m-diameter antenna. The properties are given for the frequency range of 1.0 to 30 GHz.

I. Introduction

In a recent report by this author (Ref. 1) approximate formulas were presented for calculating voltage reflection and transmission coefficients of a metallic plate perforated periodically with round holes. It was shown that the formulas were valid when the hole diameter and hole spacings were small compared to wavelength.

On the outer 47% radius of the 64-m-diameter antenna at DSS 14, perforated aluminum panels having 51% porosity and 4.763-mm ($\frac{3}{16}$ -in.) diameter holes are used as the reflective surface material. Experimental data (Refs. 2, 3) on this perforated plate material showed that the approximate formulas were accurate at S-band (2.295 GHz) and X-band (8.448 GHz) frequencies.

At K-band frequencies, the hole diameter becomes comparable in size to wavelength, and therefore the approximate formulas become inaccurate. One must therefore use more accurate formulas such as those derived by C. C. Chen (Refs. 4, 5). Chen formulated the boundary value problem for the perforated plate in terms of Floquet and orthonormal mode functions and then numerically solved the problem by use of the method of moments and a digital computer (Ref. 4). Because Chen

solves the perforated plate problem by rigorous analytical methods, his analyses apply to a large class of perforated plate problems and are not restricted to operating frequencies far below the cutoff frequency of the circular apertures.

This article presents numerical results of Chen's equations as applied to the perforated plate reflector surface material used on the 64-m-diameter antenna. The RF properties of the perforated plate are plotted for the frequency range of 1.0 to 30 GHz. Comparisons are made to the approximate formulas, which are given in the following section for convenient reference purposes.

II. Approximate Formulas

For a circular hole array having the geometry of Fig. 1 and an incident plane wave with the E-field polarized normal to the plane of incidence, the approximate expression for transmission loss is

$$\begin{aligned} (T_{dB})_{\perp} = 10 \log_{10} & \left[1 + \left(\frac{3ab\lambda_0}{2\pi d^3 \cos \theta_i} \right)^2 \right] \\ & + \frac{32t}{d} \sqrt{1 - \left(\frac{1.706d}{\lambda_0} \right)^2} \end{aligned} \quad (1)$$

where $a, b, d \ll \lambda_0$. The parameters a and b are the spacings between holes as shown in Fig. 1, d is the hole diameter, λ_0 is the free space wavelength, t is the plate thickness, and θ_i is the incidence angle.

When the incident wave is a plane wave with the E-field polarized parallel to the plane of incidence, the approximate expression is

$$(T_{dB})_{//} = 10 \log_{10} \left[1 + \left(\frac{3ab\lambda_0 \cos \theta_i}{2\pi d^3} \right)^2 \right] + \frac{32t}{d} \sqrt{1 - \left(\frac{1.706d}{\lambda_0} \right)^2} \quad (2)$$

where $a, b, d \ll \lambda_0$. It should be pointed out that the square root factor in (1) and (2) has a significant effect when λ_0 becomes comparable to d , but this factor can be omitted when $\lambda_0 \gg d$.

Other RF properties of reflector surfaces that are of interest are reflectivity loss and reflection coefficient phase angles. Assuming that the resistive losses of the plate are negligible, then these properties are given approximately by

$$(R_{dB})_{\perp} \simeq -10 \log_{10} [1 - 10^{-[(T_{dB})_{\perp}]/10}] \quad (3)$$

$$(R_{dB})_{//} \simeq -10 \log_{10} [1 - 10^{-[(T_{dB})_{//}]/10}] \quad (4)$$

$$(\psi_r)_{\perp} \simeq 180 - \tan^{-1} \left[\frac{2\pi d^3 \cos \theta_i}{3ab\lambda_0} \right] \quad (5)$$

$$(\psi_r)_{//} \simeq 180 - \tan^{-1} \left[\frac{2\pi d^3}{3ab\lambda_0 \cos \theta_i} \right] \quad (6)$$

where $(\psi_r)_{\perp}$ and $(\psi_r)_{//}$ are expressed in degrees.

The approximate formulas for perpendicular and parallel polarizations become inaccurate for incidence angles greater than 60 deg and about 40 deg, respectively. It is assumed that since $a, b, d \ll \lambda_0$, the RF properties are es-

entially independent of the incidence plane orientation angle ϕ shown in Fig. 1.

III. Numerical Results and Conclusions

As defined by the geometry in Fig. 1, the physical properties of the perforated panels on the NASA/JPL 64-m-diameter antenna are: $d = 4.763$ mm (0.1875 in.), $a = 6.350$ mm (0.250 in.), $\alpha = 60$ deg, and $t = 2.286$ mm (0.090 in.). Since the perforated panels are located on the outer 47% radius of the antenna, the incidence angle θ_i will vary only between 17.4 and 30.6 deg (Ref. 6).

Figures 2-6 show frequency characteristics of theoretical transmission losses and reflection coefficient phase angles for a plane wave incident at $\theta_i = 0, 15$, and 30 deg and for perpendicular and parallel polarizations. The frequency plot for normal ($\theta_i = 0$ deg) incidence is included for informational purposes. At a given incidence angle, the RF properties have been plotted from 1.0 GHz to a K-band frequency at which the properties no longer appear to be isotropic (i.e., independent of the incidence plane orientation angle ϕ).

Theoretical data for the frequency plots are based on Chen's formulas (Refs. 4, 5) and on the approximate formulas by this author given by Eqs. (1), (2), (5), and (6). It can be seen that the approximate formulas are useful and accurate up to about 25 GHz ($d/\lambda_0 \simeq 0.4$) but deviate significantly from Chen's data as the frequency approaches 36.9 GHz (the TE_{11} mode cutoff frequency of the circular holes). Chen's transmission loss data, which were numerically obtained by use of the Univac 1108 computer, are believed to be accurate to about ± 0.5 dB in the region far below cutoff and ± 0.1 dB or less in the region close to cutoff.

Acknowledgement

The author wishes to acknowledge the cooperation and assistance of Dr. C. C. Chen of Hughes Aircraft Company, Fullerton, Calif., Dr. C. Yeh, JPL Consultant, and P. D. Potter of the JPL Communications Elements Research Section.

References

1. Otoshi, T.Y., "Precision Reflectivity Loss Measurements of Perforated Plate Mesh Materials by a Waveguide Method," *IEEE Trans. on Instrumentation and Measurements* (Special Issue), Nov. 1972 (to be published).
2. Otoshi, T. Y., "A Study of Microwave Leakage through Perforated Flat Plates," *IEEE Trans. on Microwave Theory Tech.*, Vol. MTT-20, pp. 235-236, March 1972.
3. Otoshi, T. Y., and Woo, K., "Further Studies of Microwave Transmission through Perforated Flat Plates," in *The Deep Space Network Progress Report for September and October 1971*, Technical Report 32-1526, Vol. VI, pp. 125-129, Jet Propulsion Laboratory, Pasadena, Calif., Dec. 15, 1971.
4. Chen, C. C., "Diffraction of Electromagnetic Waves by Conducting Screen Perforated Periodically with Circular Holes," *IEEE Trans. on Microwave Theory Tech.*, Vol. MTT-19, No. 5, pp. 475-481, May 1971.
5. Chen, C. C., "Transmission of Microwave through Perforated Flat Plates of Finite Thickness," FR 72-14-530, Hughes Aircraft Co., Fullerton, Calif., May 3, 1972.
6. Otoshi, T. Y., "Antenna Noise Temperature Contributions Due to Ohmic and Leakage Losses of the DSS-14 64-m Antenna Reflector Surface," in *The Deep Space Network Progress Report for July and August 1971*, Technical Report 32-1526, Vol. V, pp. 115-119, Jet Propulsion Laboratory, Pasadena, Calif., Oct. 15, 1971.

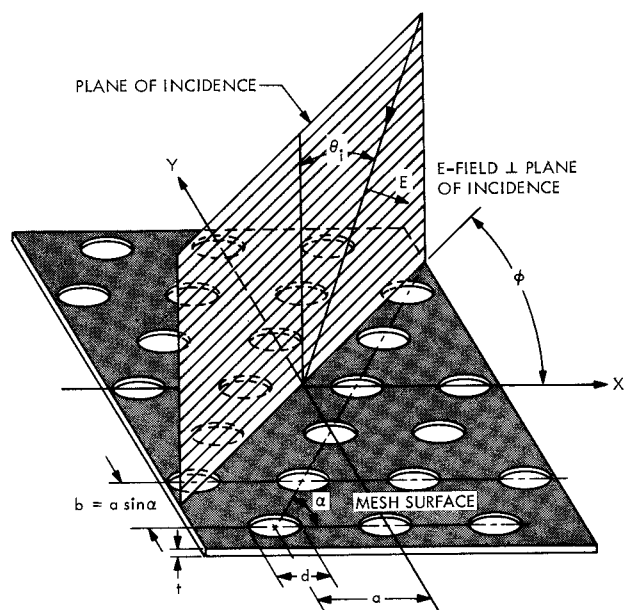


Fig. 1. Perforated plate geometry with an obliquely incident plane wave polarized with the E-field perpendicular to the plane of incidence

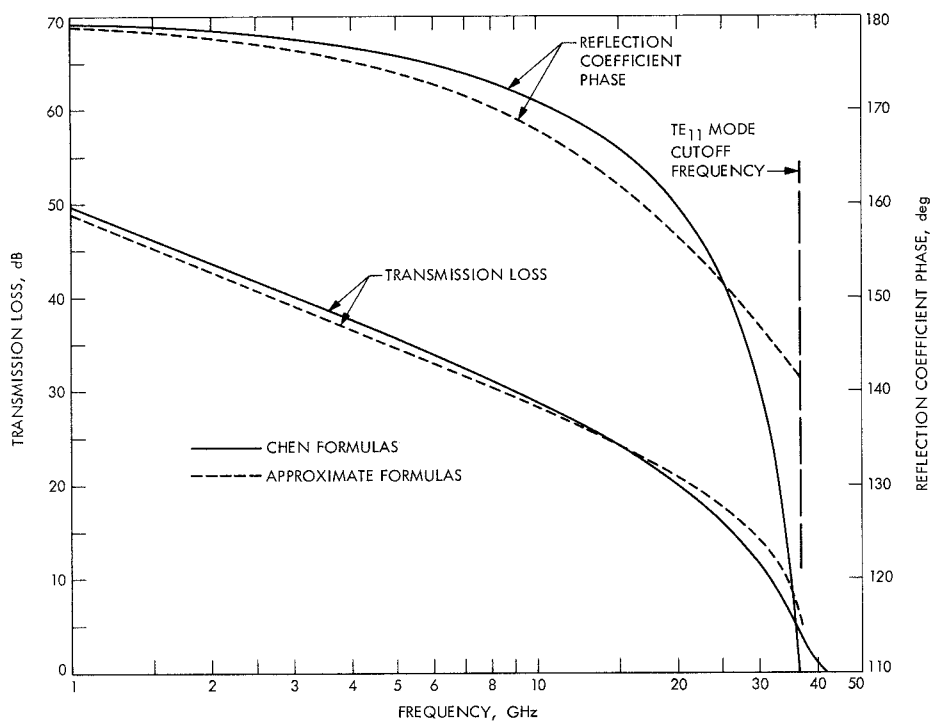


Fig. 2. 64-m-diameter antenna perforated plate transmission loss and reflection coefficient phase angle for either perpendicular or parallel polarization and 0-deg incidence angle

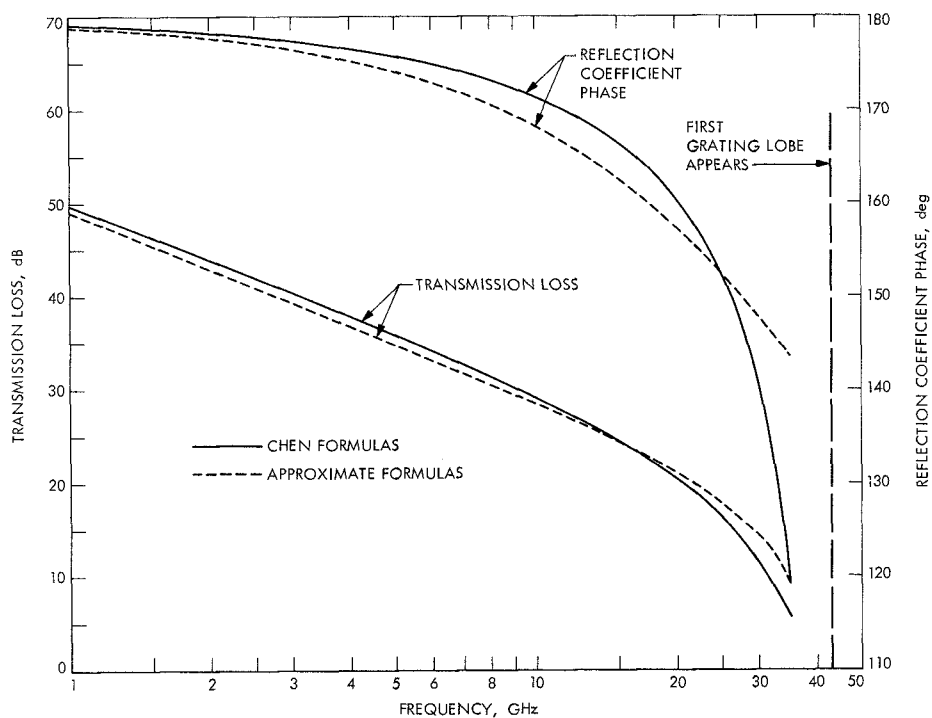


Fig. 3. 64-m-diameter antenna perforated plate transmission loss and reflection coefficient phase angle for perpendicular polarization and 15-deg incidence angle

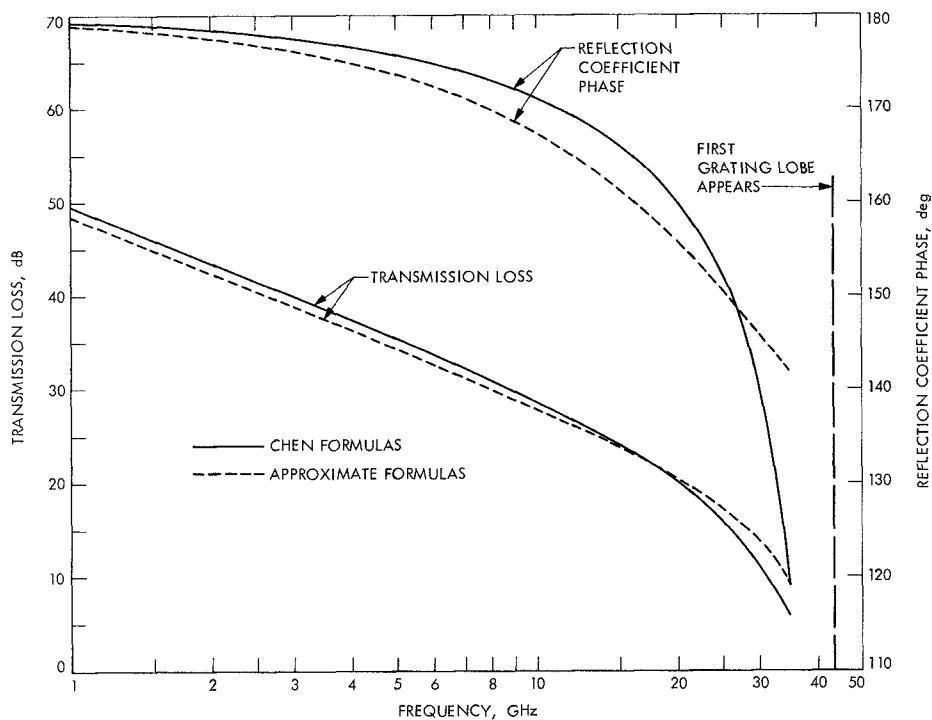


Fig. 4. 64-m-diameter antenna perforated plate transmission loss and reflection coefficient phase angle for parallel polarization and 15-deg incidence angle

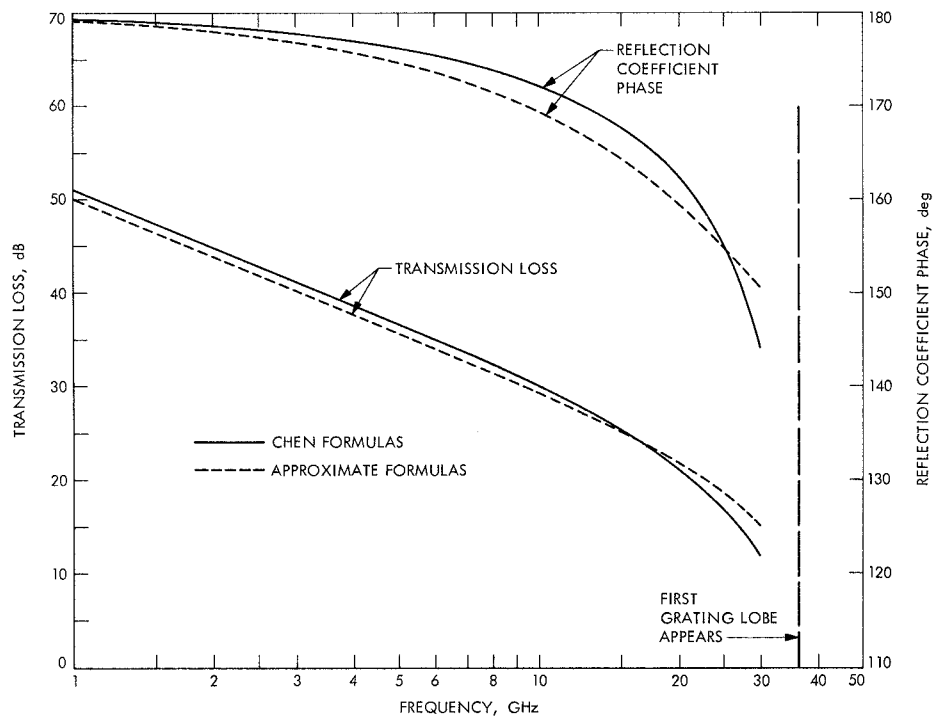


Fig. 5. 64-m-diameter antenna perforated plate transmission loss and reflection coefficient phase angle for perpendicular polarization and 30-deg incidence angle

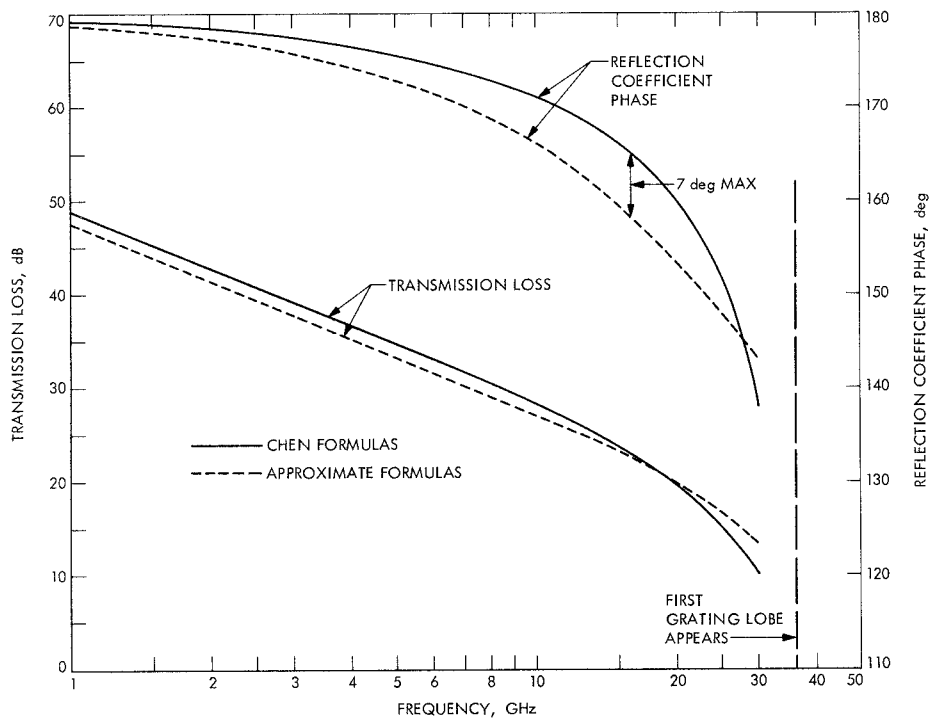


Fig. 6. 64-m-diameter antenna perforated plate transmission loss and reflection coefficient phase angle for parallel polarization and 30-deg incidence angle